XLI CILAMCE
XLI Ibero-Latin American Congress on Computational Methods in Engineering
16-19 November, 2020 FOZ DO IGUAÇU PARANÁ - BRAZIL

Attitude Tracking Control for a Quadrotor Aerial Robot Using Adaptive Sliding Modes

Jorge A. Ricardo Jr[1], Davi A. Santos[1], and Tiago Roux de Oliveira[2]

[1]*Mr. Ricardo Jr and Dr. Santos are with the Department of Mechatronics, Aeronautics Institute of Technology, São José dos Campos, SP, 12228-900, Brazil* jorgejarj@ita.br, davists@ita.br.
[2]*Dr. Oliveira is with the Department of Electronics and Telecommunication Engineering, State University of Rio de Janeiro, Rio de Janeiro, RJ, 20550-900, Brazil* tiagoroux@uerj.br.

Abstract. This work is concerned with the design and analysis of the attitude control law for a quadrotor aerial vehicle, under bounded external disturbances and model uncertainties with unknown bounds. First, the vehicle rotational kinematics and dynamics are modeled in terms of well-defined Gibbs vector and angular velocity representing the control errors. To tackle the problem, we propose a first-order multi-input adaptive sliding mode control strategy based on an adaptation law for the switching gain matrix. This adaptive gain matrix is proved to converge to its maximum bound and the existence of an ideal sliding mode is guaranteed. The main contributions are: 1) the geometric dynamic modeling in SO(3) for the attitude control error using Gibbs vector; and 2) the extension of a switching gain adaptation law originally proposed for single-input systems to a more general multi-input formulation. The method is evaluated by numerical simulations, using IMAV-M, which is a recently deployed open-source flight control simulator for multirotor aerial vehicles (MAVs). In an ideal scenario, without measurement noise (or estimation errors) and small sampling time, the method shows to be effective and easy to implement and tune.

Keywords: Adaptive sliding mode control, quadrotor, attitude control, multirotor aerial vehicle.

1 Introduction

Sliding mode control (SMC) is a popular control design approach mainly due to its simplicity and capability to make the closed-loop system insensitive to bounded matched disturbances/uncertainties [1, 2]. In this sense, the flight dynamics of multirotor aerial vehicles (MAVs) are in fact eligible for the use of SMC, since the kinematic equations describing both the translation and rotation are exactly known, while the dynamic equations contain all the uncertainties and disturbances [3]. However, SMC requires the knowledge of the disturbance bounds, which are difficult to be evaluated for MAVs, without some conservativeness.

In this context, adaptive sliding mode control (ASMC) strategies become very appealing, since they do not demand previous knowledge of the disturbance bounds. Instead, these methods either tune the switching gain of the SMC using some adaptation law [4] or adopt some disturbance estimation scheme based on the equivalent control concept [5]. In particular, the present paper is concerned with the Huang approach [4], which had its convergence proof well revisited in [6–9]. We extend this method to a multi-input formulation that fits the MAV equations of motion well. Then, in the light of the discussion raised in [6], we prove both convergence of our multi-input-based adaptive gains to its maximum bound as well as the existence of an ideal sliding mode.

Adaptive SMC with switching gain adaptation has already been applied to the flight control of fixed-rotor quadrotor MAVs [10–13]. Modirrousta and Khodabandeh [10] have propose a terminal SMC with gain adaptation in Huang's fashion for addressing the attitude control problem. Yang and Yan [11] have also considered an adaptive switching gain approach, but using a fuzzy scheduling mechanism for the gain adaptation. Based on a decoupled dynamic model of the quadrotor MAV, Nadda and Swarup [13] have applied Huang's adaptation law to design attitude and altitude controllers. Thanh and Hong [12] have employed the same modeling as in [13], but have built the adaptation law on a second-order SMC strategy. Moreover, one can find many papers on flight control of quadrotor MAVs using SMC along with either adaptive laws for estimating unknown system parameters [14–16] or disturbance observers [17, 18].

In special, we highlight that the above-cited references on flight control of MAVs are not strictly concerned

with the attitude geometry, *i.e.*, they describe the attitude control error as the difference between the desired and actual Euler angles, which has no physical meaning. In this aspect, the present work alternatively proposes to represent the attitude control error in SO(3), as done in [3, 19, 20], but using Gibbs vector instead of Euler vector (aka exponential map), Euler angles, or modified Rodrigues parameter (MRP), respectively. We argue that the Gibbs vector is an appropriate and simple choice. In summary, the present paper is concerned with the design of attitude control laws for fixed-rotor quadrotor MAVs and its main contributions are: 1) to introduce a new geometrically consistent modeling of attitude and angular velocity control errors; and 2) to propose a multi-input ASMC law that guarantees the existence of ideal sliding modes as well as switching gain boundedness. The remaining text is organized as follows. Section 2 presents the MAV modeling and details the control objectives. Section 3 develops a multi-input ASMC method for the attitude control. Section 4 evaluates the method using a simulation example. Finally, Section 5 concludes the paper.

2 Problem Statement

Subsection 2.1 presents the rotational dynamic modeling of an MAV in SO(3). Subsection 2.2 derives the rotational error dynamic equations using Gibbs vector. Section 2.3 states the control objective. For a more detailed and comprehensive modeling of an arbitrary fixed-rotor MAV in SE(3), the reader is referred to [20].

2.1 Rotational Dynamics in SO(3)

Consider a ground reference Cartesian coordinate system (CCS) $\mathcal{S}_{\mathrm{G}} \doteq \{G; \hat{x}_{\mathrm{G}}, \hat{y}_{\mathrm{G}}, \hat{z}_{\mathrm{G}}\}$ and a body-fixed CCS $\mathcal{S}_{\mathrm{B}} \doteq \{B; \hat{x}_{\mathrm{B}}, \hat{y}_{\mathrm{B}}, \hat{z}_{\mathrm{B}}\}$ as illustrated in Figure 1, along with a schematic representation of a quadrotor MAV.

Figure 1. Schematic illustration of a fixed-rotor quadrotor MAV along with the adopted CCSs.

The attitude kinematics of $\mathcal{S}_{\mathrm{B}}$ w.r.t. $\mathcal{S}_{\mathrm{G}}$ are described in SO(3) by

$$\dot{\mathbf{D}}^{\mathrm{B/G}} = -\left[\mathbf{\Omega}_{\mathrm{B}}^{\mathrm{B/G}}\times\right]\mathbf{D}^{\mathrm{B/G}}, \tag{1}$$

where $\mathbf{\Omega}_{\mathrm{B}}^{\mathrm{B/G}} \in \mathbb{R}^3$ and $\mathbf{D}^{\mathrm{B/G}} \in \mathrm{SO}(3)$ represent the MAV angular velocity and attitude, respectively.

On the other hand, using the Euler equation, the attitude dynamics are described in $\mathcal{S}_{\mathrm{B}}$ by

$$\dot{\mathbf{H}}_{\mathrm{B}} + \mathbf{\Omega}_{\mathrm{B}}^{\mathrm{B/G}} \times \mathbf{H}_{\mathrm{B}} = \mathbf{T}_{\mathrm{B}}^{c} + \mathbf{T}_{\mathrm{B}}^{d}, \tag{2}$$

where $\mathbf{H}_{\mathrm{B}} \in \mathbb{R}^3$ is the $\mathcal{S}_{\mathrm{B}}$ representation of the MAV total angular momentum, while $\mathbf{T}_{\mathrm{B}}^{c} \in \mathbb{R}^3$ and $\mathbf{T}_{\mathrm{B}}^{d} \in \mathbb{R}^3$ are the $\mathcal{S}_{\mathrm{B}}$ representation of the control and disturbance torques, respectively. Neglecting the inertia properties of the spinning part of the rotors, the $\mathcal{S}_{\mathrm{B}}$ representation of the total angular momentum can be expressed as

$$\mathbf{H}_{\mathrm{B}} = \mathbf{J}_{\mathrm{B}}\Omega_{\mathrm{B}}^{\mathrm{B/G}}, \tag{3}$$

where $\mathbf{J}_{\mathrm{B}} \in \mathbb{R}^{3\times3}$ is the inertia matrix of the airframe in $\mathcal{S}_{\mathrm{B}}$.

By replacing equation (3) into (2), we can obtain the attitude dynamic equation in the desired form:

$$\dot{\mathbf{\Omega}}_{\mathrm{B}}^{\mathrm{B/G}} = -\mathbf{J}_{\mathrm{B}}^{-1}\left[\mathbf{\Omega}_{\mathrm{B}}^{\mathrm{B/G}}\times\right]\mathbf{J}_{\mathrm{B}}\Omega_{\mathrm{B}}^{\mathrm{B/G}} + \mathbf{J}_{\mathrm{B}}^{-1}\left(\mathbf{T}_{\mathrm{B}}^{c} + \mathbf{T}_{\mathrm{B}}^{d}\right). \tag{4}$$

2.2 Error Dynamics

To keep the kinematic equation of the attitude error in the usual form (1), let us define the following attitude and angular velocity control errors, respectively:

$$\tilde{\mathbf{D}} \doteq \mathbf{D}^{\bar{\mathrm{B}}/\mathrm{B}} \in \mathrm{SO}(3) \;\text{ and }\; \tilde{\mathbf{\Omega}} \doteq \mathbf{\Omega}_{\bar{\mathrm{B}}}^{\bar{\mathrm{B}}/\mathrm{B}} \in \mathbb{R}^3, \tag{5}$$

where $\bar{\mathrm{B}}$ refers to the CCS representing the desired (or commanded) orientation for $\mathcal{S}_{\mathrm{B}}$.

Lemma 1. The attitude and angular velocity control errors can be put in the form

$$\tilde{\mathbf{D}} = \bar{\mathbf{D}}^{\mathrm{B/G}}\left(\mathbf{D}^{\mathrm{B/G}}\right)^{\mathrm{T}}, \tag{6}$$

$$\tilde{\mathbf{\Omega}} = \bar{\mathbf{\Omega}}_{\mathrm{B}}^{\mathrm{B/G}} - \tilde{\mathbf{D}}\mathbf{\Omega}_{\mathrm{B}}^{\mathrm{B/G}}, \tag{7}$$

where $\bar{\mathbf{D}}^{\mathrm{B/G}} \in \mathrm{SO}(3)$ and $\bar{\boldsymbol{\Omega}}_{\mathrm{B}}^{\mathrm{B/G}} \in \mathbb{R}^3$ represent the attitude and angular velocity commands, respectively.

Proof. Equations (6) and (7) can be immediately obtained by manipulating the control errors defined in equation (5). □

From the definition (5), the error kinematics are described in the same form as the full kinematics are represented in equation (1), *i.e.*,

$$\dot{\tilde{\mathbf{D}}} = -\left[\tilde{\boldsymbol{\Omega}}\times\right]\tilde{\mathbf{D}}. \tag{8}$$

For the design of control laws, we would rather adopt a three-dimensional parameterization of $\tilde{\mathbf{D}}$. Here, the adopted three-dimensional attitude representation is the Gibbs vector [21]:

$$\tilde{\mathbf{g}} \doteq \tilde{\boldsymbol{\varepsilon}} \tan(\tilde{\vartheta}/2), \tag{9}$$

where $\tilde{\boldsymbol{\varepsilon}} \in \mathbb{R}^3$ and $\tilde{\vartheta} \in \mathbb{R}$ are the principal Euler axis and angle, respectively, corresponding to $\tilde{\mathbf{D}}$. The direct relation between $\tilde{\mathbf{g}}$ and $\tilde{\mathbf{D}}$ is

$$\tilde{\mathbf{D}} = \frac{\left(1-\tilde{\mathbf{g}}^{\mathrm{T}}\tilde{\mathbf{g}}\right)\mathbf{I}_3 + 2\tilde{\mathbf{g}}\tilde{\mathbf{g}}^{\mathrm{T}} - 2\left[\tilde{\mathbf{g}}\times\right]}{1+\tilde{\mathbf{g}}^{\mathrm{T}}\tilde{\mathbf{g}}}, \tag{10}$$

and its inverse is

$$\tilde{\mathbf{g}} = \frac{1}{1+\operatorname{tr}\tilde{\mathbf{D}}}\begin{bmatrix}\tilde{D}_{23}-\tilde{D}_{32}\\ \tilde{D}_{31}-\tilde{D}_{13}\\ \tilde{D}_{12}-\tilde{D}_{21}\end{bmatrix}, \tag{11}$$

with $\tilde{D}_{ij}$ denoting the element of the ith row and jth column of $\tilde{\mathbf{D}}$.

From equation (9), we see that the Gibbs vector has singularities at the angles $\tilde{\vartheta} = (2i+1)\pi$ rad, $\forall i \in \mathbb{Z}$. However, since this attitude parameterization is used here to represent the attitude control error (not the full attitude), assuming that the control law to be designed will be effective, the absolute value of $\tilde{\vartheta}$ will keep much smaller than π and singularities will not be reached in practice.

Now, using the Gibbs vector parameterization, the control error kinematics are described by

$$\dot{\tilde{\mathbf{g}}} = \frac{1}{2}\left(\tilde{\mathbf{g}}\tilde{\mathbf{g}}^{\mathrm{T}} + [\tilde{\mathbf{g}}\times] + \mathbf{I}_3\right)\tilde{\boldsymbol{\Omega}}. \tag{12}$$

On the other hand, the following lemma gives the dynamic equation of the quadrotor MAV in terms of the attitude and angular velocity control errors (5).

Lemma 2. The dynamic equation (4) can be expressed as

$$\dot{\tilde{\boldsymbol{\Omega}}} = \tilde{\mathbf{D}}\mathbf{J}_{\mathrm{B}}^{-1}\left[\tilde{\mathbf{D}}^{\mathrm{T}}\left(\bar{\boldsymbol{\Omega}}_{\mathrm{B}}^{\mathrm{B/G}} - \tilde{\boldsymbol{\Omega}}\right)\times\right]\mathbf{J}_{\mathrm{B}}\tilde{\mathbf{D}}^{\mathrm{T}}\left(\bar{\boldsymbol{\Omega}}_{\mathrm{B}}^{\mathrm{B/G}} - \tilde{\boldsymbol{\Omega}}\right) + \left[\tilde{\boldsymbol{\Omega}}\times\right]\bar{\boldsymbol{\Omega}}_{\mathrm{B}}^{\mathrm{B/G}} + \dot{\bar{\boldsymbol{\Omega}}}_{\mathrm{B}}^{\mathrm{B/G}} - \tilde{\mathbf{D}}\mathbf{J}_{\mathrm{B}}^{-1}\left(\mathbf{T}_{\mathrm{B}}^{\mathrm{c}} + \mathbf{T}_{\mathrm{B}}^{d}\right). \tag{13}$$

Proof. Equation (13) can be obtained by replacing (6)–(8) into (4). □

2.3 Control Objective

Let us put the error kinematic and dynamic equations (12)–(13) into the simpler form

$$\dot{\mathbf{x}}_1 = \mathbf{f}_1(\mathbf{x}_1, \mathbf{x}_2), \tag{14}$$

$$\dot{\mathbf{x}}_2 = \mathbf{f}_2(\mathbf{x}_1, \mathbf{x}_1) + \mathbf{B}(\mathbf{x}_2)\mathbf{u} + \mathbf{B}(\mathbf{x}_2)\mathbf{d}, \tag{15}$$

by defining $\mathbf{x}_1 \doteq \tilde{\mathbf{g}}$, $\mathbf{x}_2 \doteq \tilde{\boldsymbol{\Omega}}$, $\mathbf{B}(\mathbf{x}_2) \doteq -\tilde{\mathbf{D}}\mathbf{J}_{\mathrm{B}}^{-1}$, $\mathbf{u} \doteq \mathbf{T}_{\mathrm{B}}^{\mathrm{c}}$, $\mathbf{d} \doteq \mathbf{T}_{\mathrm{B}}^{d}$,

$$\mathbf{f}_1(\mathbf{x}_1, \mathbf{x}_2) \doteq \frac{1}{2}\left(\tilde{\mathbf{g}}\tilde{\mathbf{g}}^{\mathrm{T}} + [\tilde{\mathbf{g}}\times] + \mathbf{I}_3\right)\tilde{\boldsymbol{\Omega}},$$

$$\mathbf{f}_2(\mathbf{x}_1, \mathbf{x}_2) \doteq -\mathbf{B}(\mathbf{x}_2)\left[\check{\boldsymbol{\Omega}}\times\right]\mathbf{J}_{\mathrm{B}}\check{\boldsymbol{\Omega}} + \left[\tilde{\boldsymbol{\Omega}}\times\right]\bar{\boldsymbol{\Omega}}_{\mathrm{B}}^{\mathrm{B/G}} + \dot{\bar{\boldsymbol{\Omega}}}_{\mathrm{B}}^{\mathrm{B/G}},$$

and $\check{\boldsymbol{\Omega}} \triangleq \tilde{\mathbf{D}}^{\mathrm{T}}\left(\bar{\boldsymbol{\Omega}}_{\mathrm{B}}^{\mathrm{B/G}} - \tilde{\boldsymbol{\Omega}}\right)$.

Assume that the disturbance input $\mathbf{d}$ is unknown, but it is bounded according to $|\mathbf{e}_i^{\mathrm{T}}\mathbf{d}| \leq L_i$, $i = 1, 2, 3$, where $L_i > 0, \forall i$, are unknown parameters.

Now, define the switching variable $\mathbf{s} \in \mathbb{R}^3$:

$$\mathbf{s} \doteq \mathbf{C}\mathbf{x}_1 + \mathbf{f}_1(\mathbf{x}_1, \mathbf{x}_2), \tag{16}$$

where $\mathbf{C} \in \mathbb{R}^{3\times 3}$ is a design parameter matrix.

Problem 1. The main problem of the paper is to design a feedback attitude control law for $\mathbf{u}$ so as to make $\mathbf{s}$ converge to zero in finite time, without any previous knowledge about L_i, $i = 1, 2, 3$.

To better interpret the objective of Problem 1, make $\mathbf{s} = \mathbf{0}$ in (16) to obtain $\dot{\mathbf{x}}_1 = -\mathbf{C}\mathbf{x}_1$, which represents the reduced system dynamics during the sliding mode. Clearly, if $\mathbf{C}$ is chosen as a positive-definite diagonal matrix, the equilibrium point $\mathbf{x}_1 = \mathbf{0}$ is asymptotically/exponentially stable. Therefore, we can affirm that a control law $\mathbf{u}$ which attracts $\mathbf{s}$ to zero in finite time ultimately makes $\mathbf{x}_1 \to \mathbf{0}$ asymptotically. Further, from (16), $\mathbf{x}_2 \to \mathbf{0}$ asymptotically as well. Summarily, $\mathbf{x} \doteq (\mathbf{x}_1, \mathbf{x}_2) \to \mathbf{0}$ asymptotically in spite of the presence of the disturbance input $\mathbf{d}$.

3 Control Law Design

This section presents the main results. Subsection 3.1 formulates a multi-input SMC. Subsection 3.2 presents a multi-input switching gain adaptation law.

3.1 A Multi-Input SMC Formulation

By differentiating (16) and using (14)–(15), we can obtain the dynamic equation for $\mathbf{s}$ (we omit the function independent variables for simplicity):

$$\dot{\mathbf{s}} = \mathbf{C}\mathbf{f}_1 + \frac{\partial \mathbf{f}_1}{\partial \mathbf{x}_1}\mathbf{f}_1 + \frac{\partial \mathbf{f}_1}{\partial \mathbf{x}_2}\mathbf{f}_2 + \frac{\partial \mathbf{f}_1}{\partial \mathbf{x}_2}\mathbf{B}\mathbf{u} + \frac{\partial \mathbf{f}_1}{\partial \mathbf{x}_2}\mathbf{B}\mathbf{d}. \tag{17}$$

The following lemma presents a sufficient condition for $\mathbf{s} \to \mathbf{0}$ in finite time and keep there.

Lemma 3 (Reaching Condition). The inequality

$$\mathrm{sign}^{\mathrm{T}}(\mathbf{s})\,\dot{\mathbf{s}} \leq -\frac{\beta}{\sqrt{2}}, \tag{18}$$

for any $\beta \in \mathbb{R}_{>0}$, is a sufficient condition for $\mathbf{s} = \mathbf{0}$ to be a finite-time stable equilibrium point of system (17).

Proof. Let us adopt the Lyapunov candidate function

$$V = \frac{1}{2}\left(\sum_{i=1}^{3} |s_i|\right)^2. \tag{19}$$

By deriving (19) w.r.t. time along the trajectories of $\mathbf{s}$ (governed by (17)), one can show that the finite-time convergence condition given in [22], *i.e.*, $\dot{V} \leq -\beta V^{1/2}$, can be converted into condition (18). □

The following proposition gives a multi-input SMC law which makes $\mathbf{s} \to \mathbf{0}$ in finite time, supposing, for the moment, that the disturbance bounds L_i, for $i = 1, 2, 3$, are *known*.

Proposition 1 (Multi-input SMC law). The control law

$$\mathbf{u} = -\left(\frac{\partial \mathbf{f}_1}{\partial \mathbf{x}_2}\mathbf{B}\right)^{-1}\left(\mathbf{C}\mathbf{f}_1 + \frac{\partial \mathbf{f}_1}{\partial \mathbf{x}_1}\mathbf{f}_1 + \frac{\partial \mathbf{f}_1}{\partial \mathbf{x}_2}\mathbf{f}_2 + \mathbf{K}\mathrm{sign}(\mathbf{s})\right), \tag{20}$$

where $\mathbf{K} \in \mathbb{R}^{3\times 3}$ is a constant diagonal matrix satisfying

$$\mathrm{tr}(\mathbf{K}) = \beta/\sqrt{2} + \sum_{i=1}^{3} L_i \mathbf{1}_3^{\mathrm{T}} \left|\frac{\partial \mathbf{f}_1}{\partial \mathbf{x}_2}\mathbf{B}\right| \mathbf{e}_i, \tag{21}$$

with any $\beta \in \mathbb{R}_{>0}$, guarantees a first-order sliding mode of system (14)–(15) on the switching surface $\mathbf{s} = \mathbf{0}$, in a (finite) reaching time t_r satisfying

$$t_r \leq \frac{\sqrt{2}}{\beta} \sum_{i=1}^{3} |\mathbf{e}_i^{\mathrm{T}} \mathbf{s}(0)|. \tag{22}$$

Proof. First, we need to replace the SMC law (20) into (17) to obtain:

$$\dot{\mathbf{s}} = -\mathbf{K}\mathrm{sign}(\mathbf{s}) + \frac{\partial \mathbf{f}_1}{\partial \mathbf{x}_2}\mathbf{B}\mathbf{d}. \tag{23}$$

Now, by replacing (23) into the reaching condition (18), one can show that for ensuring $\mathbf{s} \to \mathbf{0}$ in finite time, it suffices choosing $\mathbf{K}$ according to (21). On the other hand, by integrating $\dot{V} \leq -\beta V^{1/2}$ from $t = 0$ to an arbitrary t and using (19), one can obtain the reaching time bound given in (22), thus completing the proof. □

3.2 Switching Gain Adaptation

Now, let us modify the control law (20) to obtain the following ideal adaptive sliding mode control (ASMC) law:

$$\mathbf{u} = -\left(\frac{\partial \mathbf{f}_1}{\partial \mathbf{x}_2}\mathbf{B}\right)^{-1} \left(\mathbf{C}\mathbf{f}_1 + \frac{\partial \mathbf{f}_1}{\partial \mathbf{x}_1}\mathbf{f}_1 + \frac{\partial \mathbf{f}_1}{\partial \mathbf{x}_2}\mathbf{f}_2 + \mathbf{K}_a(t)\mathrm{sign}(\mathbf{s})\right), \tag{24}$$

with the switching gain $\mathbf{K}_a(t)$, still diagonal, evolving along time according to the adaptation law

$$\dot{\mathbf{K}}_a(t) = \mathbf{\Gamma}|\mathbf{s}|, \ \mathbf{K}(0) = \mathbf{K}_0 \succ 0, \tag{25}$$

where $|\mathbf{s}| \doteq [|s_1| \ |s_2| \ |s_3|]^{\mathrm{T}}$, $\mathbf{s}$ is as defined in (16), $\mathbf{K}_0$ is a given initial condition, and $\mathbf{\Gamma} \in \mathbb{R}^{3\times 3}$ is a given diagonal positive constant matrix; $\mathbf{\Gamma}$ can be chosen so as to adjust the adaptation rate for each diagonal element of $\mathbf{K}_a(t)$ independently.

The following lemma shows that the adaptive switching gain $\mathbf{K}_a(t)$ is upper-bounded by an unknown constant diagonal matrix $\bar{\mathbf{K}} \in \mathbb{R}^{3\times 3}$.

Lemma 4. Consider the switching function dynamics (17) under the ASMC law (24)–(25). It holds that there exists a positive-definite diagonal matrix $\bar{\mathbf{K}}$ such that $\bar{\mathbf{K}} - \mathbf{K}(t)$ is positive semi-definite $\forall t \geq 0$.

Proof. From (25), we see that $\dot{\mathbf{K}}_a(t) \succeq 0$, $\forall t \geq 0$. Therefore, $\mathbf{K}_a(t)$ is a non-decreasing function of t. From (25) again, we can also see that $\mathbf{K}_a(t)$ stops increasing definitely just when $\mathbf{s}$ reaches $\mathbf{0}$ definitely (to not scape again). It turns out that the value of $\mathbf{K}_a(t)$ at the time t^* when $\mathbf{s}$ reaches $\mathbf{0}$ definitely is the bound $\bar{\mathbf{K}}$ itself, thus concluding the proof. □

Now, let us replace $\mathbf{K}$ by $\mathbf{K}_a(t)$ in (23) and put the resulting equation into the reaching condition (18) to obtain:

$$\mathrm{tr}(\mathbf{K}_a(t)) \geq \frac{\beta}{\sqrt{2}} + \mathrm{sign}^{\mathrm{T}}(\mathbf{s}) \frac{\partial \mathbf{f}_1}{\partial \mathbf{x}_2}\mathbf{B}\mathbf{d}, \tag{26}$$

for any $\beta \in \mathbb{R}_{>0}$. It means that whenever condition (26) is satisfied, $\mathbf{s}$ experiences a converging motion towards the sliding surface $\mathbf{s} = 0$. In particular, the time when (26) becomes true for the last time is the one denoted by t^* in the proof of Lemma 4. Following the interpretation of Zhu and Khayati [6], we could refer to t^* as the *compensating time*.

Proposition 2. Consider the switching function dynamics (17) under the ASMC law (24)–(25). There exists a finite reaching time t_r^a such that $\mathbf{s}(t) = \mathbf{0}$, $\forall t \geq t_r^a$. Further, it holds that t_r^a satisfies

$$t_r^a \leq t^* + \frac{\sqrt{2}}{\beta} \sum_{i=1}^{3} |\mathbf{e}_i^{\mathrm{T}} \mathbf{s}(t^*)|. \tag{27}$$

Proof. The proof can be constructed in a similar way as the proof of Theorem 4.3 in [6]. □

4 Computational Example

The simulation is based on the open-source simulator IMAV-M[1], which is coded in MATLAB/Octave script in a modular fashion; for this paper, we have generated a specific fork named IMAV-M-ASMC1[2], where the proposed ASMC method is implemented on a X-shaped quadrotor MAV of 1 kg, with inertia matrix $\mathbf{J}_\mathrm{B} = \mathrm{diag}(0.015, 0.015, 0.02)$ kgm^2. For simplicity, the true attitude and angular velocity are used as feedback in place of the respective estimates. The MAV is guided to follow the position-heading waypoints $(0, 0, 1, \pi/6)$, $(5, 0, 1, \pi/6)$, and $(5, 5, 1, 0)$ (in SI units). The attitude controller is parameterized with $\mathbf{C} = \mathrm{diag}(2, 2, 2)$, $\mathbf{K}_0 = \mathrm{diag}(0.1, 0.1, 0.1)$, and $\mathbf{\Gamma} = \mathrm{diag}(0.01, 0.01, 0.01)$. The results are presented in Figure 2. It shows a smooth position trajectory following the waypoints, the control torque commands, the adaptive gains, and the attitude trajectories along the time. In the attitude plots, we see a fast and precise convergence of the true variables to the respective commands. On the other hand, the torque command is a high-frequency switching signal; it is worth noting that, even considering non-modeled actuator dynamics and using a reasonable sampling time (of 0.01 s), the chattering (in the attitude plots) is not too relevant. Finally, we can see that the switching gains keep growing, since s cannot converge exactly to zero in a non-ideal scenario. Further analysis will appear in a future paper, considering sensor noise and more challenging flight scenarios.

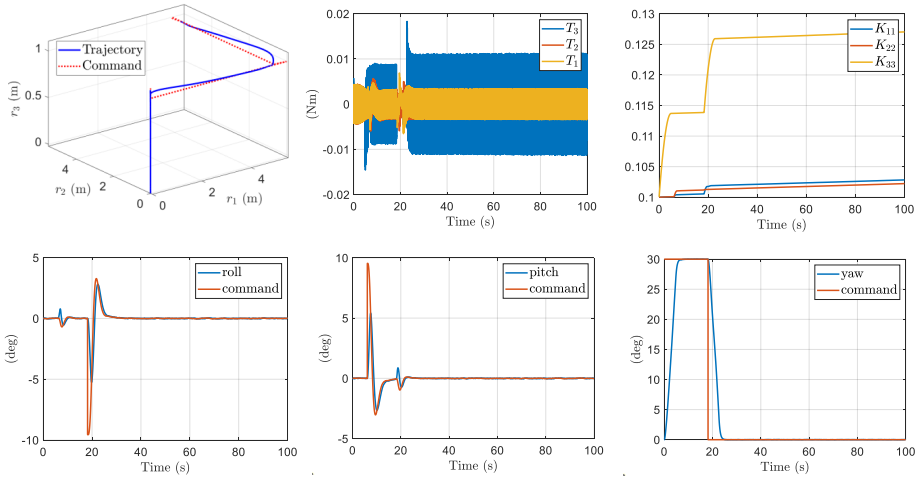

Figure 2. Simulation results.

5 Conclusions

The paper solved the attitude control problem for quadrotor MAVs using an ideal adaptive multi-input SMC with adaptive switching gain. Sliding mode existence and gain boundedness are both ensured. A simulation example showed the effectiveness and promising performance of the method. In a future work, the proposed controller will be extended to a real ASMC design and will be fully evaluated using simulation and experiments.

ACKNOWLEDGMENT

The authors would like to thank the Sao Paulo Research Foundation (FAPESP), for the financial support (2019/05334-0). The first author is grateful to EMBRAER and ITA, for the doctorate scholarship under the Academic-Industrial Graduate Program (DAI). The second author is grateful for the support of CNPq/Brazil (302637/2018-4).

Authorship statement. This section is mandatory and should be positioned immediately before the References section. The text should be exactly as follows: The authors hereby confirm that they are the sole liable persons responsible for the authorship of this work, and that all material that has been herein included as part of the present paper is either the property (and authorship) of the authors, or has the permission of the owners to be included here.

[1] See `https://github.com/daviasantos/IMAV-M`.
[2] It is available here: `https://github.com/daviasantos/IMAVMASMC1`.

References

[1] Slotine, J. E. & Li, W., 1990. *Applied Nonlinear Control*. Prentice Hall.
[2] Shtessel, Y., Edwards, C., Fridman, L., & Levant, A., 2014. *Sliding Mode Control and Observation*. Springer, New York.
[3] Silva Jr, A. L. & Santos, D. A., 2020. Fast nonsingular terminal sliding mode flight control for multirotor aerial vehicles. *IEEE Transactions on Aerospace and Electronic Systems*.
[4] Huang, Y., Kuo, T., & Chang, S., 2008. Adaptive sliding-mode control for nonlinear systems with uncertain parameters. *IEEE Transactions on Systems, Man, and Cybernetics, Part B (Cybernetics)*, vol. 38, n. 2, pp. 534–539.
[5] Lee, H. & Utkin, V., 2007. Chattering suppression methods in sliding mode control systems. *Annual Reviews in Control*, vol. 31, n. 2, pp. 179–188.
[6] Zhu, J. & Khayati, K., 2016. Adaptive sliding mode control convergence and gain boundedness revisited. *International Journal of Control*, vol. 89, n. 4, pp. 801–814.
[7] Plestan, F., Shtessel, Y., Brégeault, V., & Poznyak, A., 2010. New methodologies for adaptive sliding mode control. *International Journal of Control*, vol. 83, n. 9, pp. 1907–1919.
[8] Utkin, V. I. & Poznyak, A. S., 2013. *Advances in Sliding Mode Control - Concept, Theory and Implementation*, pp. 21–53. Lecture Notes in Control and Information Sciences. Springer-Verlag Berlin Heidelberg.
[9] Cong, B., Chen, Z., & Liu, X., 2014. On adaptive sliding mode control without switching gain overestimation. *International Journal of Robust and Nonlinear Control*, vol. 24, n. 3, pp. 515–531.
[10] Modirrousta, A. & Khodabandeh, M., 2015. A novel nonlinear hybrid controller design for an uncertain quadrotor with disturbances. *Aerospace Science and Technology*, vol. 45, pp. 294–308.
[11] Yang, Y. & Yan, Y., 2016. Attitude regulation for unmanned quadrotors using adaptive fuzzy gain-scheduling sliding mode control. *Aerospace Science and Technology*, vol. 54, pp. 208–217.
[12] Thanh, H. L. N. N. & Hong, S. K., 2018. Quadcopter robust adaptive second order sliding mode control based on pid sliding surface. *IEEE Access*, vol. 6, pp. 66850–66860.
[13] Nadda, S. & Swarup, A., 2018. On adaptive sliding mode control for improved quadrotor tracking. *Journal of Vibration and Control*, vol. 24, n. 14, pp. 3219–3230.
[14] Escareño, J., Salazar, S., Romero, H., & Lozano, R., 2013. Trajectory control of a quadrotor subject to 2d wind disturbances robust-adaptive approach. *Journal of Intelligent & Robotic Systems*, vol. 70, pp. 51–63.
[15] Mofid, O. & Mobayen, S., 2018. Adaptive sliding mode control for finite-time stability of quad-rotor uavs with parametric uncertainties. *ISA Transactions*, vol. 72, pp. 1–14.
[16] Labbadi, M. & Cherkaoui, M., 2020. Robust adaptive nonsingular fast terminal sliding-mode tracking control for an uncertain quadrotor uav subjected to disturbances. *ISA Transactions*, vol. 99, pp. 290–304.
[17] Ma, D., Xia, Y., Shen, G., Jia, Z., & Li, T., 2018. Flatness-based adaptive sliding mode tracking control for a quadrotor with disturbances. *Journal of the Franklin Institute*, vol. 355, n. 14, pp. 6300–6322.
[18] Ahmed, N. & Chen, M., 2018. Sliding mode control for quadrotor with disturbance observer. *Advances in Mechanical Engineering*, vol. 10, n. 7, pp. 1–16.
[19] Shi, X., Zhang, Y., & Zhou, D., 2017. Almost-global finite-time trajectory tracking control for quadrotors in the exponential coordinates. *IEEE Transactions on Aerospace and Electronic Systems*, vol. 53, n. 1, pp. 91–100.
[20] Santos, D. A. & Cunha Jr., A., 2019. Flight control of a hexa-rotor airship: Uncertainty quantification for a range of temperature and pressure conditions. *ISA Transactions*, vol. 93, pp. 268–279.
[21] Markley, F. L. & Crassidis, J. L., 2014. *Fundamentals of Spacecraft Attitude Determination and Control*. Space Technology Library. Springer-Verlag, New York.
[22] Bhat, S. P. & Bernstein, D. S., 2000. Finite-time stability of continuous autonomous systems. *SIAM J. Control. Optim.*, vol. 38, pp. 751–766.